REFERENCES AND NOTES

1. H. V. Crouse, *Genetics* **45**, 1429 (1960); A. Razin and H. Cedar, *Cell* **77**, 473 (1994).
2. S. Zemel, M. S. Bartolomei, S. M. Tilghman, *Nature Genet.* **2**, 61 (1992).
3. D. Kitsberg *et al.*, *Nature* **364**, 459 (1993).
4. M. Lalande, *Nature Genet.* **8**, 5 (1994); R. D. Nicholls, J. H. M. Knoll, M. G. Butler, S. Karam, M. Lalande, *Nature* **342**, 281 (1989); S. Malcolm *et al.*, *Lancet* **337**, 694 (1991).
5. J. H. M. Knoll, S.-D. Cheng, M. Lalande, *Nature Genet.* **6**, 41 (1994).
6. J. M. LaSalle and M. Lalande, *ibid.* **9**, 386 (1995).
7. Y. Hiraoka *et al.*, *J. Cell Biol.* **120**, 591 (1993); B. Judd, *Cell* **53**, 841 (1988); V. Pirrotta, *BioEssays* **12**, 409 (1990); K. D. Tartof and S. Henikoff, *Cell* **65**, 201 (1991).
8. N. Kleckner and B. M. Weiner, *Cold Spring Harbor Symp. Quant. Biol.* **58**, 553 (1993).
9. Human T lymphocytes were isolated and flow-sorted on the basis of DNA content as described previously, except "early S" includes the S_1 and S_2 fractions, whereas "late S" includes the S_3 and S_4 fractions (*6*). A modified FISH protocol was developed that minimizes alterations in the normal spatial organization of the nucleus (*21*). Cells were adhered for 5 min to poly-D-lysine–coated slides, fixed 15 min in 4% paraformaldehyde and 1% methanol in phosphate-buffered saline (PBS), washed twice in 0.3 M glycine and PBS, permeabilized for 10 min in 0.5% Tween and 0.2 N HCl, washed twice in 2× saline sodium citrate (SSC), denatured 3 min in 70% formamide and 2× SSC, washed twice in 0.5% Tween and PBS and twice in 2× SSC at 4°C, then hybridized and washed as previously described (*6*) without detection steps. D15Z1 (pHSR) and D12Z3 (pA12H8, ATCC) were directly labeled by nick translation with Cy3- and Cy5-labeled deoxycytidine triphosphate (Biological Detection), respectively, and nuclei were counterstained with YOPRO (Molecular Probes). Nuclei were imaged by a Molecular Dynamics CLSM Multiprobe 2001 with an Ar/Kr laser. Imagespace software (Molecular Dynamics) was used for scanning, analysis, and projection images. Nuclei were densely distributed (Fig. 1A), and we selected clusters of 6 to 20 nuclei by using only the DNA counterstain filter to avoid bias in selection. Optical sections were scanned with a 60× objective at a 0.21, 0.21, 0.29 voxel resolution and a total image size of 512 by 512 pixels. Hybridization efficiency was 85% (number of nuclei with two red and two green signals out of the total number of nuclei scanned, in an average of four representative experiments). The *x*, *y*, and *z* coordinates were defined at the center of each hybridization signal and used to measure 3D distance by a mouse-driven cursor.
10. J. M. LaSalle and M. Lalande, unpublished results.
11. P. Emmerich *et al.*, *Exp. Cell Res.* **181**, 126 (1989); J. P. Lewis, H. J. Tanke, A. K. Raap, G. C. Beverstock, H. Kluin-Nelemans, *Hum. Genet.* **92**, 577 (1993); L. Manuelidis, *Science* **250**, 1533 (1990).
12. M. Ferguson and D. C. Ward, *Chromosoma* **101**, 557 (1992).
13. Mean nuclear diameter was 8 μm with a range of 6 to 12 μm, as determined by the 3D object count feature of Imagespace software. No substantial differences in nuclear diameter were observed between different cell cycle fractions.
14. The distance of 2.0 μm was chosen on the basis of a comparison of the graph of late S phase lymphocytes to that of premeiotic yeast (*22*). The degree of nonrandomness was similar, but the scale of the graphs was different because the diameter of yeast nuclei was ~5 μm, whereas lymphocytes are ~6 to 12 μm (*13*). Pairing in premeiosis and meiosis may involve a tighter association between homologs, or yeast chromosomes may have fewer spatial constraints than chromosomes in higher eukaryotes, thus explaining the difference in actual distances.
15. Single-copy probes were labeled with biotin or digoxigenin and detected with anti-digoxigenin-fluorescein (green) and Cy3-avidin (red) as previously described (*9*), but with 0.5% Tween in the last wash. To increase cell density, we fixed and washed the cells in suspension, then cytocentrifuged them at 55*g* for 4 min before permeabilization. There was no detectable change in nuclear shape by a *z* scan. Hybridization efficiencies were 75%. Separation of sister chromatid FISH signals at replicated sites was observed infrequently as a result of the low resolution of pixel aquisition (0.21 μm^2), lack of physical spreading of DNA by the altered FISH protocol, and larger probe size (centromeric repeats and 80- to 120-kb P1 clones). In the infrequent cases where replication doublets were observed, the measurement was taken at the point between the two signals. Source numbers for P1 clones at Genomesystems are as follows: GABRB3/A5, 2269; D15S113, 6343; D13S104, 6269; D15S128, 7207; and D15S46 (ATCC).
16. T. Haaf and M. Schmid, *Exp. Cell Res.* **192**, 325 (1991).
17. S. A. Lesko, D. E. Callahan, M. E. LaVilla, Z.-P. Wang, P. O. P. Ts'o, *Ibid.* **219**, 499 (1995); L. Manuelidis, *Hum. Genet.* **71**, 288 (1985).
18. P. A. Leighton, J. R. Saam, R. S. Ingram, C. L. Stewart, S. M. Tilghman, *Genes Dev.* **9**, 2079 (1995); P. A. Leighton, R. S. Ingram, J. Eggenschwiler, A. Efstratiadis, S. M. Tilghman, *Nature* **375**, 34 (1995); J. S. Sutcliffe *et al.*, *Nature Genet.* **8**, 52 (1994); K. Buiting *et al.*, *ibid.* **9**, 395 (1995).
19. P. H. Gunaratne, M. Nakao, D. H. Ledbetter, J. S. Sutcliffe, A. C. Chinault, *Genes Dev.* **9**, 808 (1995).
20. J.-Y. Tsai and L. M. Silver, *Genetics* **129**, 1159 (1991).
21. R. T. O'Keefe, S. C. Henderson, D. L. Spector, *J. Cell Biol.* **116**, 1095 (1992).
22. B. M. Weiner and N. Kleckner, *Cell* **77**, 977 (1994).
23. Patient G1478 in W. P. Robinson *et al.*, *Eur. J. Hum. Genet.* **1**, 280 (1993).
24. Patient AS136 in A. Bottani *et al.*, *Am. J. Med. Genet.* **51**, 35 (1994).

25. We thank W. Robinson, K. Hirschorn, S. Orkin, A. Bottani, B. Horsthemke, R. Wharton, J. Holden, B. White, M. Higgins, A. Flint, K. Glatt, Q. M. Liu, H. Lidov, J. Wagstaff, and L. M. Kunkel for their help and important contributions to this work. Supported by Howard Hughes Medical Institute and NIH grant RO1-NS30628.

7 December 1995; accepted 6 March 1996

Amelioration of Vascular Dysfunctions in Diabetic Rats by an Oral PKC β Inhibitor

Hidehiro Ishii, Michael R. Jirousek, Daisuke Koya, Chikako Takagi, Pu Xia, Allen Clermont, Sven-Erik Bursell, Timothy S. Kern, Lawrence M. Ballas, William F. Heath, Lawrence E. Stramm, Edward P. Feener, George L. King*

The vascular complications of diabetes mellitus have been correlated with enhanced activation of protein kinase C (PKC). LY333531, a specific inhibitor of the β isoform of PKC, was synthesized and was shown to be a competitive reversible inhibitor of PKC β_1 and β_2, with a half-maximal inhibitory constant of ~5 nM; this value was one-fiftieth of that for other PKC isoenzymes and one-thousandth of that for non-PKC kinases. When administered orally, LY333531 ameliorated the glomerular filtration rate, albumin excretion rate, and retinal circulation in diabetic rats in a dose-responsive manner, in parallel with its inhibition of PKC activities.

The major causal factor in the development of retinopathy and nephropathy in diabetes mellitus is hyperglycemia (*1*). One theory (*2*) has attributed the adverse effect of hyperglycemia to the activation of PKC, a family of serine-threonine kinases that regulate many vascular functions, including contractility, hemodynamics, and cellular proliferation (*3*, *4*). PKC activity is increased in the retina, aorta, heart, and renal glomeruli of diabetic animals, probably because of an increase in de novo synthesis of diacylglycerol (DAG), a major endogenous activator of PKC (*2*, *5*, *6*). Our observation that the PKC β_2 isoenzyme is preferentially activated in the retina, heart, and aorta of diabetic rats (*2*) led us to propose that the abnormal activation of PKC β_2 may cause some of the diabetic vascular complications (*5*). To test this hypothesis, we synthesized an orally effective PKC inhibitor that was PKC β selective and evaluated its ability to ameliorate vascular dysfunctions in diabetic rats.

On the basis of the structures of known PKC inhibitors (*7*, *8*), we performed an extensive screening to identify and optimize a PKC β–selective inhibitor. A panel of eight cloned human PKC isoenzymes (α, β_1, β_2, γ, δ, ε, ζ, and η) was used to profile the selectivity of the inhibitor, with DAG used as an activator (*3*, *8*). The macrocyclic bis(indolyl)maleimide structure (LY333531) was found to inhibit PKC β selectively (Scheme 1). LY333531 inhibited PKC β_1 and β_2 with a half-maximal inhibitory constant (IC_{50}) of 4.7 and 5.9 nM, respectively, whereas for other PKC isoenzymes except η, the IC_{50} was 250

H. Ishii, D. Koya, C. Takagi, P. Xia, A. Clermont, S.-E. Bursell, E. P. Feener, G. L. King, Research Division, Joslin Diabetes Center, Department of Medicine, Brigham and Women's Hospital and Harvard Medical School, 1 Joslin Place, Boston, MA 02215, USA.
M. R. Jirousek, W. F. Heath, L. E. Stramm, Lilly Laboratories, Indianapolis, IN 46285, USA.
T. S. Kern, Department of Ophthalmology, University of Wisconsin, Madison, WI 53706, USA.
L. M. Ballas, Sphinx Pharmaceutical, Durham, NC 27707, USA.
*To whom correspondence should be addressed.

nM or greater (Table 1). For PKC η, the IC_{50} was 52 nM. For other adenosine triphosphate (ATP)–dependent kinases studied, the IC_{50} was $>10^5$ nM, and for calcium calmodulin kinase, it was 8×10^3 nM. Kinetic analysis with Lineweaver-Burk and Dixon plots showed that LY333531 was a competitive inhibitor for ATP, with an inhibition constant K_i of 2 nM for PKC β_1. In contrast, staurosporine was not isoform selective among α, β_1, β_2, γ, δ, ε, and η.

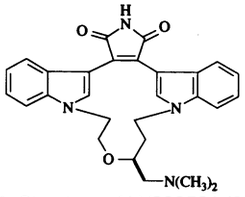

Scheme 1. Structure of LY333531 (*22*).

The specificity of LY333531 was also evaluated in vascular smooth muscle cells that overexpressed PKC β_2. We used phosphorylation of PKC α and β_2 as a marker of PKC activation and inhibition by LY333531, because the activation of these PKC enzymes correlates with their phosphorylation (*9*). We substantiated this finding with purified PKC α and β_2; LY333531 (10 and 20 nM) inhibited the phosphorylation of PKC β_2 but not of PKC α (Fig. 1A). When aortic smooth muscle cells were exposed to phorbol 12-myristate 13-acetate (PMA) for 30 min, both PKC α and β_2 were activated, as measured by a fivefold increase in their translocation to the membrane fraction (*10*). This increase in PKC translocation correlated with increased phosphorylation of both PKC α and β_2 (Fig. 1B). LY333531 (10 nM) inhibited the autophosphorylation or transphosphorylation (*9*) of PKC β_2 by up to 70%, as measured by immunoprecipitation with PKC β_2–specific antibodies, but did not inhibit PKC α (Fig. 1B). These results indicate that LY333531 selectively inhibits PKC β_2 both in vitro and in cultured cells at similar concentrations.

To evaluate whether LY333531 affected activation of PKC in the retina and the renal glomeruli, we studied the effects of three oral doses—0.1, 1.0, and 10.0 mg per kilogram of body weight (mg/kg)—in nondiabetic and streptozotocin-induced diabetic rats. The plasma concentration of LY333531 at the highest dose was 5.7 and 19 nM for control and diabetic rats, respectively (*11*). None of the three doses affected body weight, amount of blood glucose, or mean blood pressure in either group of rats (Table 2). Even at the highest dose of LY333531, the amounts of plasma glucose in the diabetic rats (380 ± 27 mg/dl) were greater than those in the nondiabetic rats (100 ± 5 mg/dl). In addition, the amounts of glycosylated hemoglobin in the diabetic rats (12.3 ± 1.4%, untreated) were not affected by 8 to 10 weeks of treatment with LY333531 at 10 mg/kg (12.1 ± 0.4%).

One potential cause of PKC activation in diabetic vascular tissue is the increased amount of palmitate-labeled DAG derived from glucose metabolism (*12*). We therefore measured total amounts of DAG in the retina and renal glomeruli of diabetic and nondiabetic rats. The amounts of DAG in the

Table 1. Selectivity of LY333531 and staurosporine for PKC isoenzymes and other kinases. Each of the human PKC enzymes was partially purified from Sf9 cells expressing the individual PKC enzymes. PKC activity was assayed by quantitating the incorporation of ^{32}P from γ-[^{32}P]ATP into either histone (type IIIS) or myelin basic protein (*20*).

Kinase	IC_{50} (nM)	
	LY333531	Staurosporine
PKC α	360	45
PKC β_1	4.7	23
PKC β_2	5.9	19
PKC γ	300	110
PKC δ	250	28
PKC ε	600	18
PKC ζ	$>10^5$	$>1.5 \times 10^3$
PKC η	52	5
Cyclic AMP kinase	$>10^5$	100
Ca^{2+}-calmodulin kinase	8×10^3	4
Casein kinase	$>10^5$	1.4×10^4
Src tyrosine kinase	$>10^5$	1

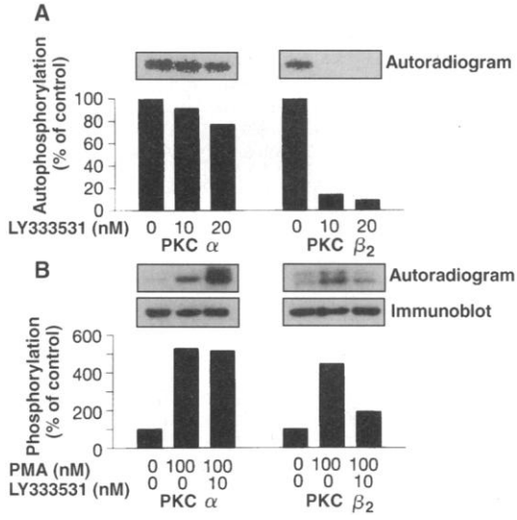

Fig. 1. Effect of LY333531 on phosphorylation of PKC α and β_2. (**A**) Purified PKC α (33.8 μg/ml) and PKC β_2 (81.1 μg/ml) prepared from the baculovirus expression system (*23*) were incubated with LY333531 for 20 min at 30°C in the presence of Ca^{2+} (1 mM), phosphatidylserine (100 μg/ml), and DAG (1.3 μg/ml). The reaction was started by the addition of ATP (30 μM) with γ-[^{32}P]ATP (30 μCi per 100 nmol). After 3 min, the reaction was terminated by addition of Laemmli's sample buffer. PKC was resolved by SDS–polyacrylamide gel electrophoresis (SDS-PAGE), and autophosphorylation was quantitated by scanning densitometry of the autoradiograph. (**B**) Confluent rat aortic smooth muscle cells overexpressing PKC β_2 were labeled with [^{32}P]orthophosphate (1 mCi/ml) in phosphate-free Dulbecco's modified Eagle's medium for 3 hours at 37°C and treated with 10 nM LY333531 for 30 min. The cells were then stimulated with 100 nM PMA for 30 min. The culture medium was removed, and 0.5 ml of 20 mM tris-HCl (pH 7.5), 1% Triton X-100, 2 mM EDTA, 0.5 mM EGTA, 2 mM phenylmethylsulfonyl fluoride, leupeptin (100 μg/ml), aprotinin (50 μg/ml), 50 mM NaF, 2 mM Na_3VO_4, and 1 mM dithiothreitol was added to the cells. The solubilized cells were centrifuged at 15,000*g* for 10 min at 4°C, and the supernatants were immunoprecipitated by incubation with antibodies to PKC α or β_2 overnight at 4°C and bound to protein A–Sepharose beads. The precipitated proteins were analyzed by SDS-PAGE followed by autoradiography and immunoblotting. The results are the means of two different experiments.

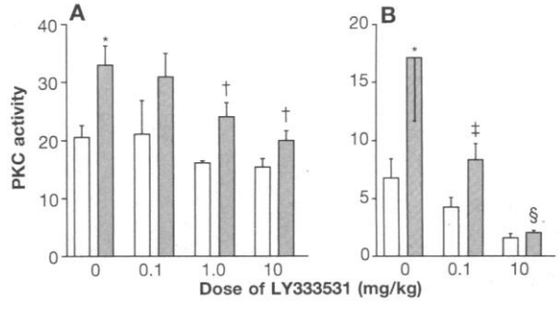

Fig. 2. Effect of LY333531 on PKC activity (in picomoles per minute per milligram of protein) in glomeruli (**A**) and in retina (**B**) isolated from nondiabetic rats (open columns) and diabetic rats (shaded columns). After 2 weeks of treatment with LY333531, the rats were killed with CO_2 gas and their retinas were dissected. Glomeruli samples were isolated from kidneys by differential sieving (*21*). PKC activities in glomeruli and retina were measured as in (*24*), except that PKC activity was calculated by subtracting the phosphorylation in the absence of PKC-specific peptide substrate (Arg-Lys-Arg-Thr-Leu-Arg-Arg-Leu) (*25*) from that in the presence of the peptide. Validation of PKC activity was done by stimulating retina and glomeruli with PMA, which activated PKC equally by either in situ assay or the translocation assay (PKC activation was 2 and 1.6 times baseline in the retina and glomeruli, respectively). The results are expressed as mean ± SE. Statistical analysis: *$P < 0.01$ versus nondiabetic rats without LY333531; †$P < 0.05$, ‡$P < 0.01$, and §$P < 0.001$ versus diabetic rats without LY333531 (Student-Newman-Keuls test).

retina and glomeruli in the diabetic rats were 149% and 135%, respectively, of the amounts in the nondiabetic rats (Table 2). LY333531 (10 mg/kg) did not affect the increase in the amount of DAG in the retina or the glomeruli of diabetic rats relative to nondiabetic controls. PKC activity was increased in both the retina and glomeruli of diabetic rats (Fig. 2). PKC β_2 is the predominant activated PKC isoenzyme in the retina, aorta, and heart (*2*, *5*) and was also found to be the predominant activated isoenzyme in the glomeruli of diabetic rats (*13*).

The PKC activities in the retina and glomeruli of the diabetic rats were 254% and 161%, respectively, of those in the nondiabetic rats (Fig. 2). LY333531 (0.1 mg/kg) reduced PKC activity to normal rates in the retina of the diabetic rats but did not significantly affect PKC activity in the nondiabetic rats (Fig. 2B). In the retina of the nondiabetic rats, PKC activity decreased from 6.8 ± 1.6 to 1.5 ± 0.4 pmol/min per milligram of protein at the highest dose of LY333531 (10 mg/kg). In the renal glomeruli (Fig. 2A), significant reduction of PKC activity was observed with high doses of LY333531 (1.0 and 10 mg/kg). In contrast to the effect observed in the retina, treatment with PKC inhibitor at 0.1 mg/kg did not reduce the activation of PKC in the renal glomeruli of diabetic rats. Additionally, in the glomeruli of nondiabetic rats, no significant decreases in PKC activity were noted even at the highest dose of LY333531 (10 mg/kg). The different responses of retina and renal glomeruli could be the result of different maximum amounts of LY333531 that these tissues can accumulate. In addition, the lack of effect of LY333531 in nondiabetic rats suggests that PKC β may not be significantly activated in these tissues under normal circumstances.

Table 2. Characterization of rats after 2 weeks of treatment with LY333531. Male Sprague-Dawley rats weighing 240 to 260 g were injected intraperitoneally with streptozotocin at 65 mg/kg. Diabetes was confirmed by testing blood glucose on the following day. The rats were randomly assigned to eight feeding groups. The low-, medium-, and high-dose groups were fed rat chow mixed with LY333531 at doses of 0.1, 1.0, and 10 mg/kg, respectively. Blood pressure was measured with a tail cuff. For the measurement of total amounts of DAG, the retinas and kidneys were dissected from the rats, and glomeruli samples were then isolated from kidneys by differential sieving (*21*). Total lipid was extracted and total DAG was determined by an enzymatic assay with DAG kinase (*5*). Animal protocols were approved by the Joslin Diabetes Center Animal Care Committee. Values are expressed as mean ± SD.

Dose of LY333531	*n*	Body weight (g)	Blood glucose (mg/dl)	Mean blood pressure (mmHg)	Kidney weight (g)	Total DAG	
						Glomeruli (nmol/mg protein)	Retina (pmol/mg wet weight)
				Nondiabetic rats			
None	9	373 ± 19	100 ± 10	119 ± 7	2.9 ± 0.2	2.0 ± 0.8	138 ± 36
Low	6	378 ± 15	109 ± 9	124 ± 9	3.0 ± 0.3		
Medium	6	390 ± 17	110 ± 10	118 ± 8	3.1 ± 0.2		
High	7	359 ± 21	100 ± 5	119 ± 9	2.8 ± 0.1	1.7 ± 0.8	102 ± 54
				Diabetic rats			
None	9	312 ± 27†	381 ± 51†	115 ± 8	3.3 ± 0.5	2.7 ± 0.5*	205 ± 57*
Low	6	323 ± 33†	380 ± 30†	121 ± 9	3.2 ± 0.2		
Medium	6	318 ± 17†	368 ± 48†	114 ± 8	3.2 ± 0.3		
High	9	297 ± 31†	380 ± 27†	125 ± 10	3.0 ± 0.5	2.8 ± 1.1*	203 ± 65*

*$P < 0.05$, †$P < 0.001$ versus nondiabetic rats without LY333531 (Student-Newman-Keuls test).

To determine whether LY333531 affected vascular functions in the diabetic rats, we measured the renal glomerular filtration rate (GFR), urinary albumin excretion rate (AER), and retinal mean circulation time (MCT). Among the two earliest manifestations of renal abnormality are an increase in GFR, which indicates increased intraglomerular pressure (*14*, *15*), and an increase in urinary AER, which has been associated with the development of diabetic nephropathy (*14*, *16*). Hyperglycemia may alter vascular regulation intraglomerularly, possibly through interactions with angiotensin and endothelin (*17*). To characterize renal function in nondiabetic and diabetic rats, we measured renal plasma flow (RPF) and GFR by means of *p*-aminohippuric acid (PAH) clearance and inulin clearance, respectively (Fig. 3A). GFR was found to be 3.0 ± 0.2 ml/min in nondiabetic rats and was unaffected by LY333531. In diabetic rats, GFR increased significantly to 4.6 ± 0.4 ml/min. Treatment with high doses (1.0 and 10 mg/kg) but not low doses (0.1 mg/kg) of LY333531 returned the increased GFR in diabetic rats to normal. The dose-response curve of LY333531 in normalizing GFR paralleled its inhibitory effect on PKC activity (Fig. 2A). In the same group of nondiabetic and diabetic rats, RPF was also measured, but no significant changes were observed. The calculated filtration fraction (GFR/RPF) was found to be 0.29 ± 0.01 for the nondiabetic rats and 0.37 ± 0.04 for the diabetic rats, an increase of 28% (Fig. 3B). Treatment with LY333531 at 1.0 and 10 mg/kg returned the filtration fraction to normal (0.29 ± 0.03 and 0.31 ± 0.01, respectively), but this effect was not observed at a dose of 0.1 mg/kg. Urinary AER was significantly higher in the diabetic rats (11.7 ± 3.1 mg/day) than in the nondiabetic rats (1.6 ± 0.5 mg/day) (Fig. 3C). Treatment with LY333531 (10 mg/kg) for 8 weeks significantly decreased urinary AER in the diabetic rats to 4.9 ± 1.6 mg/day. The improvement of urinary AER by LY333531 may be associated with a correction of renal hemodynamics (*14*, *15*) and may ameliorate the development of nephropathy (*18*).

Diabetic rats show an increase in retinal MCT (*19*), possibly as a result of changes in

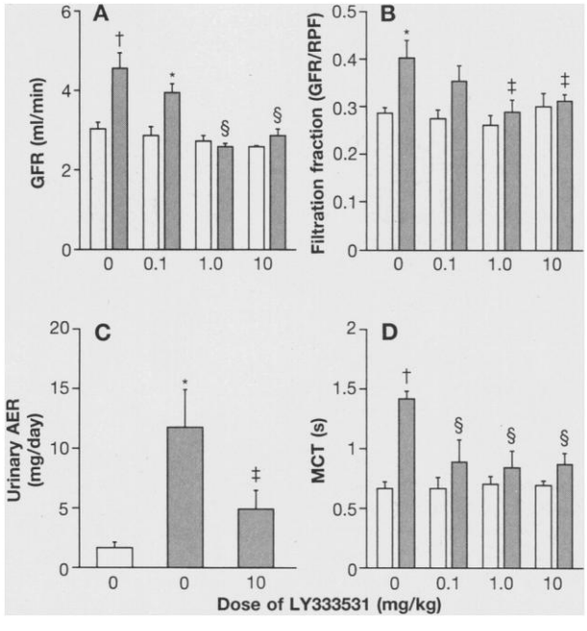

Fig. 3. Effect of LY333531 on renal and retinal vascular functions and urinary AER in nondiabetic rats (open columns) and diabetic rats (shaded columns). (**A** and **B**) Renal GFR and filtration fraction (*26*) after 2 weeks of treatment with LY333531. (**C**) Urinary AER after 8 weeks of treatment with LY333531. Urine samples were collected from 10 nondiabetic rats, 9 untreated diabetic rats, and 8 diabetic rats treated with LY333531 (10 mg/kg), and urinary AER was measured by ELISA (*27*). (**D**) Retinal MCT measured by video fluorescein angiograms (*19*) after 2 weeks of treatment with LY333531. The results are expressed as mean ± SE. Statistical analysis: *$P < 0.01$ and †$P < 0.001$ versus nondiabetic rats without LY333531; ‡$P < 0.05$ and §$P < 0.001$ versus diabetic rats without LY333531 (Student-Newman-Keuls test).

microvascular resistance, and this increase is associated with the activation of PKC. Nondiabetic and diabetic rats had MCT values of 0.67 and 1.40 s, respectively (Fig. 3D). Oral treatment with 0.1, 1.0, and 10 mg/kg of LY333531 reduced MCT in the diabetic rats to 0.89, 0.84, and 0.87 s, respectively, but had no effect on nondiabetic rats. Again, the dose-response curve of LY333531 in ameliorating retinal MCT paralleled its inhibitory effect on PKC β activity (Fig. 2B). Our results demonstrate that in a rat model, an orally administered PKC β inhibitor can be effective in an isoenzyme-specific manner, without apparent toxicity, and can correct some of the vascular dysfunctions associated with diabetes mellitus. Hence, abnormal activation of PKC, in particular its β isoenzymes, may underlie some of these vascular complications of diabetes.

REFERENCES AND NOTES

1. Diabetes Control and Complication Trial Research Group, *N. Engl. J. Med.* **329**, 977 (1993).
2. T. Inoguchi *et al., Proc. Natl. Acad. Sci. U.S.A.* **89**, 11059 (1992).
3. Y. Nishizuka, *Science* **258**, 607 (1992).
4. H. Rasmussen, J. Forder, I. Kojima, A. Scriabine, *Biochem. Biophys. Res. Commun.* **122**, 776 (1984); C. Caramelo, P. Tsai, R. W. Schrier, *Biochem. J.* **254**, 625 (1988).
5. T. Shiba *et al., Am. J. Physiol.* **265**, E783 (1993).
6. P. A. Craven and F. R. DeRubertis, *J. Clin. Invest.* **83**, 1667 (1989).
7. T. Tamaoki *et al., Biochem. Biophys. Res. Commun.* **135**, 397 (1986); D. Toullec *et al., J. Biol. Chem.* **266**, 15771 (1991); E. Andrejauskas-Buchdunger and U. Regenass, *Cancer Res.* **52**, 5353 (1992).
8. M. R. Jirousek *et al., Bioorg. Med. Chem. Lett.*, in press.
9. F. E. Mitchell, R. M. Marais, P. J. Parker, *Biochem. J.* **261**, 131 (1989); S. Ohno, Y. Konno, Y. Akita, A. Yano, K. Suzuki, *J. Biol. Chem.* **265**, 6296 (1990); J. Zhang, L. Wang, J. Petrin, W. R. Bishop, R. W. Bond, *Proc. Natl. Acad. Sci. U.S.A.* **90**, 6130 (1993); J. Zhang, L. Wang, J. Schwartz, R. W. Bond, W. R. Bishop, *J. Biol. Chem.* **269**, 19578 (1994); E. M. Dutil, L. M. Keranen, A. A. DePaoli-Roach, A. C. Newton, *ibid.*, p. 29359.
10. P. Xia, R. M. Kramer, G. L. King, *J. Clin. Invest.* **96**, 733 (1995).
11. The serum half-life of LY333531 was ~6 hours. The main metabolite was a desmethylated product that in vitro was similar to LY333531 in potency and specificity of PKC β inhibition.
12. P. A. Craven, C. M. Davidson, F. R. DeRubertis, *Diabetes* **39**, 667 (1990); T. Inoguchi *et al., Am. J. Physiol.* **267**, E369 (1994); P. Xia *et al., Diabetes* **43**, 1122 (1994).
13. H. Ishii and G. L. King, unpublished data. PKC was partially purified from glomeruli of diabetic and nondiabetic rats (*2*), and PKC isoforms were measured by immunoblotting. PKC β_2 in the membranous fraction of diabetic rats was significantly increased (204 ± 43%) versus nondiabetic rats. No significant increases were observed with PKC isoenzymes α, δ, or ε in the same fraction.
14. T. H. Hostetter, H. G. Rennke, B. M. Brenner, *Am. J. Med.* **72**, 375 (1982).
15. M. P. O'Donnell, B. L. Kasiske, W. F. Keane, *FASEB J.* **2**, 2339 (1988).
16. C. E. Mogensen and C. K. Christensen, *N. Engl. J. Med.* **311**, 89 (1984).
17. M. Haneda *et al., Kidney Int.* **44**, 518 (1993); R. D. Hurst *et al., Diabetes* **44**, 759 (1995).
18. C. E. Mogensen, *N. Engl. J. Med.* **310**, 356 (1984); *Kidney Int.* **31**, 673 (1987).
19. S.-E. Bursell, A. C. Clermont, T. Shiba, G. L. King, *Curr. Eye Res.* **11**, 287 (1992).
20. The reaction mixture (250 μl) contained 30 μg of phosphatidylserine and 0.5 μg of DAG in 20 mM Hepes (pH 7.5), 10 mM $MgCl_2$, 100 μM EGTA (with or without 94 μM $CaCl_2$, depending on the PKC isoenzyme), histone (200 μg/ml) or myelin basic protein (250 μg/ml), compound in dimethyl sulfoxide (DMSO) or DMSO alone at four different concentrations, 30 μM ATP with γ-[^{32}P]ATP, and the PKC isoenzyme. Reaction time was 10 min at 30°C. Incubations were terminated with 500 μl of 25% trichloroacetic acid and 100 μl of bovine serum albumin (BSA) (1 mg/ml). The reaction mixture was filtered onto glass fiber mats with a Tom Tec filtration unit. Radioactivity was measured with a liquid scintillation counter.
21. H. Ohashi *et al., Regul. Pept.* **48**, 9 (1993).
22. LY333531 was synthesized by a cyclization reaction and converted to the dimethylamine derivative (*8*). (*S*)-1-*tert*-Butyldiphenylsilyloxy-2-(2-iodoethyloxy)-4-iodobutane was slowly added to a dimethylformamide slurry containing cesium carbonate and 3,4-bis(3,3′-indolyl)-1-methyl-pyrrole-2,5-dione. This isolated product was hydrolyzed and converted to the *NH*-maleimide with removal of the silyl protecting group. The resulting alcohol was converted to the mesylate and displaced with dimethyl amine to give the macrocyclic bis(indolyl)maleimide, LY333531.
23. A. Toker *et al., J. Biol. Chem.* **269**, 32358 (1994).
24. L. E. Heasley and G. L. Johnson, *J. Biol. Chem.* **264**, 8646 (1989); B. Williams and R. W. Schrier, *Diabetes* **41**, 1464 (1992).
25. I. Yasuda *et al., Biochem. Biophys. Res. Commun.* **166**, 1220 (1990).
26. The rats were anesthetized with thiopental sodium (50 mg/kg intraperitoneal). Catheters were then surgically inserted in the left carotid artery (for blood sampling), the left jugular vein (for infusion), and the urinary bladder (for collection of urine). Inulin (0.6%) and PAH (1.5%) in normal saline were infused at a rate of 6.0 ml/hour for 30 min, followed by a sustained infusion of 2.0 ml/hour throughout the experiment. After 60 min, two clearance studies (each 30 min) were performed in succession. The concentrations of inulin and PAH were measured by the anthrone method [W. H. Waugh, *Clin. Chem.* **23**, 639 (1977)] and the calorimetric technique [H. W. Smith, N. Finkelstein, L. Aliminosa, B. Crawford, M. Grabor, *J. Clin. Invest.* **24**, 388 (1945)], respectively. GFR and RPF were determined by inulin and PAH clearance, respectively, and the filtration fraction was calculated from the ratio of GFR to RPF.
27. Enzyme-linked immunosorbent assay (ELISA) plates were coated with 50 μl of sheep antibody to rat albumin immunoglobulin G (IgG) (10 μg/ml) at 4°C overnight and blocked with 100 μl of 1% BSA for 1 hour at 37°C. The plates were incubated with 50 μl of standard rat albumin or urine samples and then with 50 μl of peroxidase-conjugated sheep antibody to rat albumin IgG for 1 hour at 37°C. Finally, the reaction was started by incubation with 100 μl of 0.11 M Na_2HPO_4 and 0.04 M citric acid (pH 5.5) containing *o*-phenylenediamine dihydrochloride (1 mg/ml) and 0.05% hydrogen peroxide. After 2 min, the reaction was terminated by adding 100 μl of 3M H_2SO_4, and absorbance at 492 nm was measured with a spectrophotometer. The assay range was 3 to 250 ng/ml, and the intra- and inter-assay coefficients of variation were 2.4% and 6.5%, respectively.

28. Supported by National Eye Institute grant NEI-05110-11 and Diabetes and Endocrinology Research Center grant NIDDK-36836, and partially supported by Lilly Pharmaceutical, Inc. We thank J. Davis and K. Kalter for help with the in vitro kinase assays and L. Balmat for excellent secretarial assistance.

14 September 1995; accepted 13 March 1996

A Mouse Model of Familial Hypertrophic Cardiomyopathy

Anja A. T. Geisterfer-Lowrance, Michael Christe, David A. Conner, Joanne S. Ingwall, Frederick J. Schoen, Christine E. Seidman, J. G. Seidman*

A mouse model of familial hypertrophic cardiomyopathy (FHC) was generated by the introduction of an $Arg^{403} \rightarrow Gln$ mutation into the α cardiac myosin heavy chain (MHC) gene. Homozygous $\alpha MHC^{403/403}$ mice died 7 days after birth, and sedentary heterozygous $\alpha MHC^{403/+}$ mice survived for 1 year. Cardiac histopathology and dysfunction in the $\alpha MHC^{403/+}$ mice resembled human FHC. Cardiac dysfunction preceded histopathologic changes, and myocyte disarray, hypertrophy, and fibrosis increased with age. Young male $\alpha MHC^{403/+}$ mice showed more evidence of disease than did their female counterparts. Preliminary results suggested that exercise capacity may have been compromised in the $\alpha MHC^{403/+}$ mice. This mouse model may help to define the natural history of FHC.

FHC is an autosomal dominant condition characterized by unexplained ventricular hypertrophy with myocyte and myofibrillar disarray. Affected individuals typically experience shortness of breath, angina, and palpitations, but many are asymptomatic. Sudden death, heart failure, and stroke are the most serious consequences of the disease (*1*, *2*). Molecular genetic studies have demonstrated that mutations in the β cardiac MHC can cause FHC (*2*, *3*). However, FHC is clinically diverse even among affected family members who share the same β cardiac MHC mutation (*4*). For example, some affected individuals die during childhood, whereas others survive into their sixth to seventh decade (*1*, *2*). The mechanisms by which mutations in the β cardiac MHC cause hypertrophic cardiomyopathy, and the roles of physical activity, environment, and modifying genes in the clinical heterogeneity of the disease, are poorly understood.

A missense mutation, $Arg^{403} \rightarrow Gln$